

This is an Open Access document downloaded from ORCA, Cardiff University's institutional repository: <https://orca.cardiff.ac.uk/id/eprint/95519/>

This is the author's version of a work that was submitted to / accepted for publication.

Citation for final published version:

Muenzner, Julienne K, Biersack, Bernhard, Albrecht, Alexander, Rehm, Tobias, Lacher, Ulrike, Milius, Wolfgang, Casini, Angela, Zhang, Jing-Jing, Ott, Ingo, Brabec, Viktor, Stuchlikova, Olga, Andronache, Ion C, Schuppan, Detlef, Kaps, Leonard and Schobert, Rainer 2016. Ferrocenyl-coupled n-heterocyclic carbene complexes of gold(i): a successful approach to multinuclear anticancer drugs. *Chemistry - a European Journal* 22 (52), pp. 18953-18962. 10.1002/chem.201604246

Publishers page: <http://dx.doi.org/10.1002/chem.201604246>

Please note:

Changes made as a result of publishing processes such as copy-editing, formatting and page numbers may not be reflected in this version. For the definitive version of this publication, please refer to the published source. You are advised to consult the publisher's version if you wish to cite this paper.

This version is being made available in accordance with publisher policies. See <http://orca.cf.ac.uk/policies.html> for usage policies. Copyright and moral rights for publications made available in ORCA are retained by the copyright holders.



Supporting Information

Ferrocenyl-Coupled N-Heterocyclic Carbene Complexes of Gold(I): a Successful Approach to Multinuclear Anticancer Drugs

Julienne K. Muenzner,^a Bernhard Biersack,^a Alexander Albrecht,^a Tobias Rehm,^a Ulrike Lacher,^a Wolfgang Milius,^b Angela Casini,^{c,d} Jing-Jing Zhang,^e Ingo Ott,^e Viktor Brabec,^{f,g} Olga Stuchlikova,^{f,g} Ion C. Andronache,^h Leonard Kaps,ⁱ Detlef Schuppan,^{i,j} and Rainer Schobert^{a,*}

^a*Organic Chemistry Laboratory, University of Bayreuth, Universitätsstraße 30, 95447 Bayreuth, Germany*

^b*Lehrstuhl für Anorganische Chemie I Universität Bayreuth, Universitätsstraße 30, 95447 Bayreuth Germany*

^c*Department of Pharmacokinetics, Toxicology and Targeting, Research Institute of Pharmacy, University of Groningen, Antonius Deusinglaan 1, 9713 AV Groningen, The Netherlands*

^d*School of Chemistry, Cardiff University, Main Building, CF10 3AT Cardiff, United Kingdom*

^e*Institute of Medicinal and Pharmaceutical Chemistry, Technische Universität Braunschweig, Beethovenstrasse 55, 38106 Braunschweig, Germany*

^f*Institute of Biophysics, Academy of Sciences of the Czech Republic, v.v.i., Kralovopolska 135, CZ-61265 Brno, Czech Republic*

^g*Department of Biophysics, Faculty of Science, Palacky University, 17. listopadu 12, CZ-77146 Olomouc, Czech Republic*

^h*Research Centre for Integrated Analysis and Territorial Management, University of Bucharest, 1 Nicolae Balcescu Blvd., district 1, 010055, Bucharest, Romania*

ⁱ*Institute of Translational Immunology, University Medical Center of the Johannes Gutenberg University Mainz, Langenbeckstrasse 1, 55131 Mainz, Germany*

^j*Division of Gastroenterology Beth Israel Deaconess Medical Center, Harvard Medical School Boston, US.*

^{*}Corresponding author. E-mail: Rainer.Schobert@uni-bayreuth.de; Fax: +49 (0)921 552671; Phone: +49 (0)921 552679.

TOC

Cell lines and culture conditions	S1
Growth inhibition (MTT) assay	S1
Cellular Iron Accumulation	S2
Measurement of the partition coefficient	S2
Fluorescence Labeling of F-Actin and Tubulin	S2
Cell Cycle Analysis	S3
Wound Healing Assay	S3
Generation of ROS (NBT assay)	S3
JC-1 Mitochondrial Membrane Potential Assay	S3
Mass spectrometric selenocysteine binding studies	S4
Cyclic voltammetry of 7b	S7
References	S8
NMR spectra	S9

Cell lines and culture conditions: The human melanoma cell line 518A2 was obtained from the Department of Radiotherapy, Medical University of Vienna (Austria).¹⁻³ The Panc-1 pancreatic carcinoma cell line (CRL-1469TM), the DLD-1 colorectal adenocarcinoma cells (CCL-221TM), and the CCD-18Co human fibroblasts (CRL-1459TM) were obtained from the American Type Culture Collection (ATCC). All other cancer cell lines as well as the human umbilical vein endothelial cells (HUVEC) were purchased from the German Centre of Biological Materials (DSMZ), Braunschweig, Germany. All cells were cultured in Dulbecco's modified Eagle's medium (DMEM) containing 10% fetal bovine serum (FBS), 1% antibiotic-antimycotic, and 250 mg/mL gentamycin (all from Gibco) at 37 °C in a humidified atmosphere of 95% air and 5% CO₂, apart from HUVEC, which were cultured in EGM-2 medium (Lonza) supplemented with 5% FBS at 37 °C, 10% CO₂ and 90% humidity. Only mycoplasma-free cultures were used.

Growth inhibition (MTT) assay: The antiproliferative activity of complexes **7a**, **7b**, **8**, and **10** was determined using 3-(4,5-dimethylthiazol-2-yl)-2,5-diphenyltetrazolium bromide (MTT; Roth) that is reduced to a violet formazan in viable cells.⁴ All cancer cells (5000 cells per well) were seeded and grown for 24 h on 96-well microplates. The KB-V1/Vbl cells were optionally pretreated with 24 µM of verapamil (24 h). Incubation of cells following addition of the test compounds (dilution series of 10 mM stock solutions in dimethylformamide (DMF) ranging from 5×10⁻⁶ to 100 µM in H₂O) was continued for 72 h. Solvent controls were treated identically. A 0.05% solution of MTT (50 µL/well) in phosphate buffered saline (PBS) was added to the cells after centrifugation (300 g, 5 min, 4 °C) and removal of the medium. After another 2 h of incubation the microplates were centrifuged and the supernatant MTT solution was discarded. A 10% solution of sodium dodecylsulfate (SDS) in DMSO containing 0.6% acetic acid was added to dissolve the precipitated water-insoluble formazan crystals (25 µL/well). The microplates were incubated overnight to ensure a complete dissolution of the violet formazan. The absorbance at 570 nm and 630 nm was measured using an automatic TECAN Infinite[®] F200 plate reader. The test compounds' concentrations at which viable cells were reduced to 50% (IC₅₀ values) are presented as means ± S.D. of four independent experiments (solvent controls set to 100% viable cells). The antiproliferative effect of the complexes on vascular endothelial cells and their selectivity towards cancer cells with respect to non-malignant cells was analogously assessed by MTT assays using HUVEC and CCD-18Co fibroblasts, respectively. However, these non-malignant cells were seeded at a higher density of 10,000 cells/well due to their slower proliferation rates.

Cellular Iron Accumulation: Cellular uptake of complexes **7a**, **7b**, **8**, and **10** was measured using HCT-116 colon carcinoma cells. The cells were seeded on 100 mm tissue culture dishes (1.5×10^6 cells/dish in 10 mL of growth medium). After 24 h of incubation, the cells were treated with the complexes (each 0.5 μ M) for 24 h (the concentrations were verified by measuring the iron content in the growing medium by ICP-MS). The attached cells were harvested by trypsinization and the cell pellets were washed twice with ice-cold PBS (4 °C). The pellets were digested by using a microwave based acid digestion system (CEM MARS and 11 M HCl) to give a fully homogenized solution. The final iron content in the samples was determined by ICP-MS. Values are means \pm S.D. of three independent experiments.

Measurement of the Partition Coefficient: To determine the partition coefficient (P) the shake flask method was used. The complexes **7a**, **7b**, **8**, and **10** were separately dissolved in milli-Q water at a concentration of 0.5 μ M and the solutions were filtered through 0.2 μ m sterile filters. These solutions were mixed with an equal amount of 1-octanol by vortexing for 24 h at room temperature to establish the partition equilibrium. The aqueous layer was carefully separated from the 1-octanol layer for iron analysis. Iron was quantified from water aliquots taken from aqueous samples before (0.5 μ M concentration) and after partition by ICP-MS. The partition coefficients were calculated using the equation $\log P = \log ([\text{Fe}]_{1\text{-octanol}} / [\text{Fe}]_{\text{water}})$ and are presented as means \pm S.D. of three independent experiments.

Fluorescence Labeling of F-Actin and Tubulin: Effects of gold complexes **8** and **10** on the organization of F-actin and microtubules in HUVEC and 518A2 melanoma cells were examined by fluorescence microscopy. Cells were cultured on glass coverslips to 75% confluence. For HUVEC, the glass coverslips were pretreated with 1M HCl/EtOH. Following treatment with **8** (500 nM), **10** (250 nM) or vehicle for 24 h, cells were fixed with 4% formalin (in PBS) for 20 min at room temperature, washed with PBS and permeabilized with 1% BSA, 0.1% Triton X-100 (in PBS) for 30 min. For F-actin staining fixed cells were stained (37 °C, 1 h) with AlexaFluor® 488 Phalloidin (1 U/mL, Invitrogen). To visualize tubulin, fixed and permeabilized cells were treated first with primary antibodies against alpha-tubulin (anti-alpha-tubulin mouse mAb, 5 μ g/mL, Invitrogen) and then for 1 h at room temperature with Alexa Fluor® 488 conjugated sec. antibodies (goat anti-mouse IgG-AlexaFluor®-488 conjugate, 4 μ g/mL, Invitrogen). Nuclei were counterstained with DAPI (1 μ g/mL) in PBS, at room temperature for 5 min, before coverslips were washed in PBS and mounted with ProLong Gold Antifade reagent (Invitrogen). Effects were analyzed using an Axioplan fluorescence microscope with a 40 \times objective lens (Zeiss, AxioCam MRm).

Cell Cycle Analysis: 518A2 cells ($5 \times 10^4/\text{mL}$) were cultured in 6-well plates for 24 h and then treated with 500 nM of **8** or 250 nM of **10** for 24 h. Solvent controls (DMF) were treated identically. After fixation with 70% EtOH at 4 °C, the cells were incubated with propidium iodide (PI; Roth) staining solution (50 $\mu\text{g/mL}$ PI, 0.1% sodium citrate, 50 $\mu\text{g/mL}$ RNase A in PBS) for 30 min at 37 °C. The fluorescence intensity of 10,000 single cells was measured at $\lambda_{\text{em}} = 620 \text{ nm}$ ($\lambda_{\text{ex}} = 488 \text{ nm}$ laser source) using a Beckman Coulter Cytomics FC 500 flow cytometer and analyzed (CXP Analysis, Beckman Coulter) for the fractions of cells in G1, S and G2/M phase. The percentage of apoptotic cells was assessed from sub-G1 peaks. Experiments in triplicate.

Wound Healing Assay: 518A2 melanoma cells ($1 \times 10^5/\text{mL}$) were seeded on 24-well plates and grown to a sub-confluent monolayer. A narrow artificial wound was created by scraping off a strip of cells with a 20–200 μL plastic tip. The medium was replaced before cells were treated with 500 nM each of **8** or **10**, or vehicle (DMF) for up to 48 h. The wound-healing process was monitored with a light microscope (Axiovert 135 with a 10 \times objective lens, Zeiss, AxioCam MRc5) after 24 h and 48 h of exposure to the test compounds. The size of the wound was measured at three different positions (top, middle, bottom) of each microscopy image using Adobe Photoshop CS6 (Version 13.01), the mean width of the wound was calculated for each documented time point (0 h, 24 h and 48 h), and the percentage of wound healing over time was determined as means \pm S.D. of at least three experiments.

Generation of ROS (NBT assay): The adherent 518A2 cells ($1 \times 10^5/\text{mL}$) were plated in 96-well tissue culture plates and test compounds **8** and **10** were added at various concentrations (250 nM, 500 nM and 1 μM) after 24 h of incubation at 37 °C, 5% CO₂ and 95% humidity). Incubation of cells following treatment with the test compounds was continued for another 24 h. A 0.1% solution of NBT (50 $\mu\text{L}/\text{well}$) in PBS was added to the cells after centrifugation (300 g, 5 min, 4 °C) and removal of the medium. After another 4 h of incubation the microplates were centrifuged and the supernatant NBT solution was discarded. The precipitated blue diformazan crystals were dissolved in 50 μL of 2M KOH and 65 μL DMSO for 30 min. The absorbance at 630 and 405 nm was measured using an automatic TECAN plate reader (TECAN Infinite® F200). For each substance the experiment was carried out twice in triplicate.

JC-1 Mitochondrial Membrane Potential Assay: The effect of complexes **8** and **10** on the mitochondrial transmembrane potential ($\Delta\psi_{\text{m}}$) was evaluated using Cayman's JC-1

Mitochondrial Membrane Potential Assay Kit. The experiment was carried out according to the manufacturer's protocol.⁵⁻⁷ Briefly, the adherent 518A2 cells ($1 \times 10^5/\text{mL}$) were seeded in black 96-well tissue culture plates and test compounds **8** or **10** were added after 24 h of incubation at 37 °C, 5% CO₂ and 95% humidity. Incubation of the cells, following addition of the test compounds in different concentrations (250 nM, 500 nM and 1 μM), was continued for 24 h. Then, 5 μL of the JC-1 staining solution were added per well, cells were incubated with this fluorescent dye for 20 min, and after two washing steps the fluorescence intensities of JC-1 aggregates (red) and monomers (green) were measured at 590 ± 20 nm and 535 ± 25 nm, respectively. The ratio of the fluorescence intensity of JC-1 aggregates to the fluorescence intensity of JC-1 monomers is indicative for the cells' health and the induction of apoptosis. Control cells were set to 100% of cells with an intact mitochondrial membrane potential. The assay was carried out twice in triplicate for each complex.

Mass spectrometric selenocysteine binding studies: Complexes **7b**, **8**, and **10** were incubated for 30 min with seleno-L-cysteine, freshly prepared *in situ* from selenocystine and DTT (1:4). The resulting mixtures were analysed by HRMS using an Orbitrap system in ESI⁺ mode according to a protocol by Casini *et. al.*⁸ The following pictures are not to uniform scale!

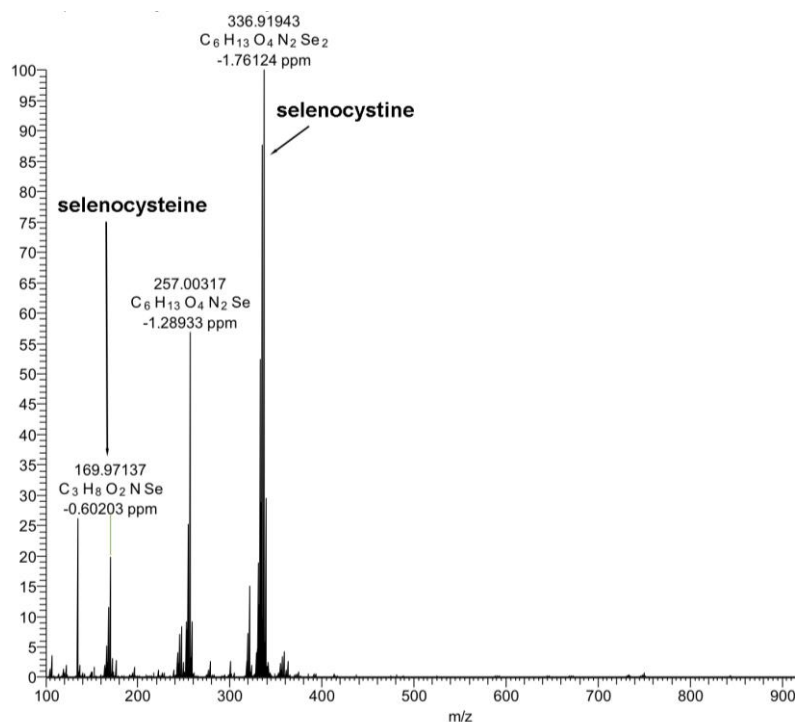


Fig. S 1: 1:4 Mixture of selenocystine and DTT after 30 min at r.t.

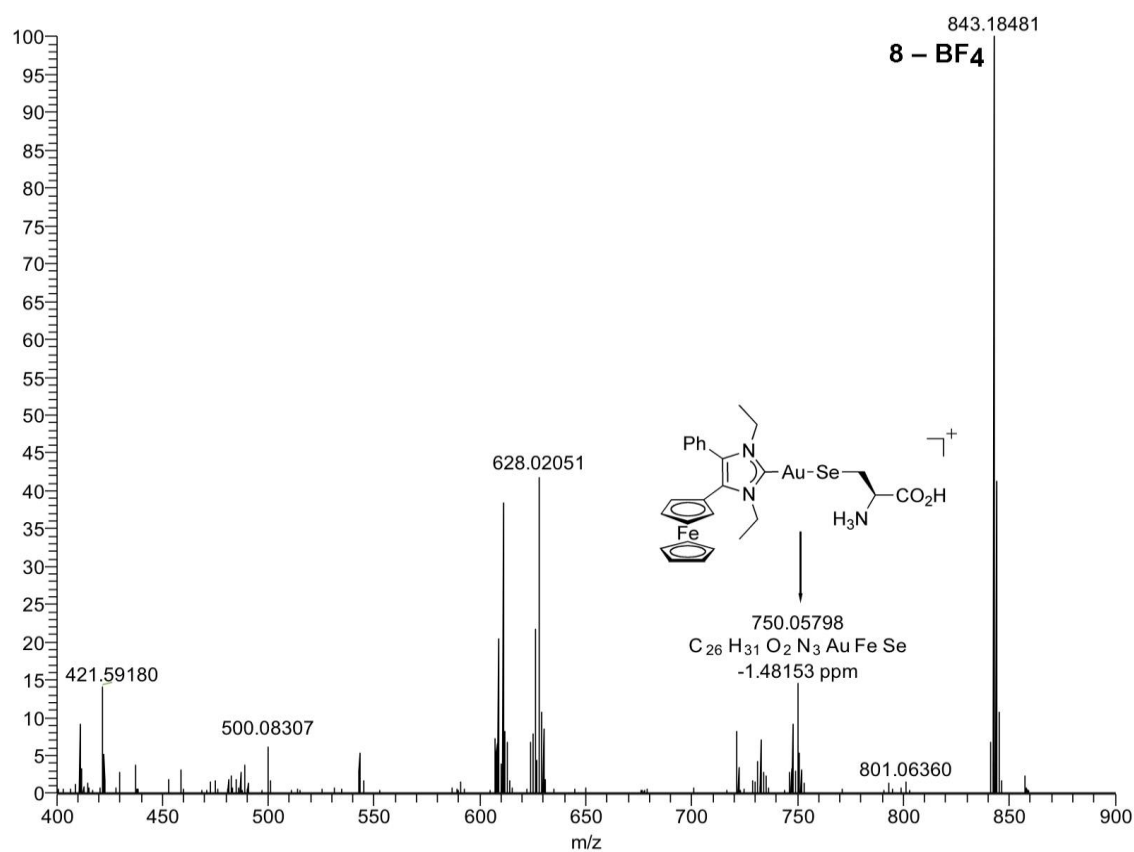


Fig. S 2: Mixture with selenocysteine prepared as above incubated with complex **8** for 30 min at r.t.

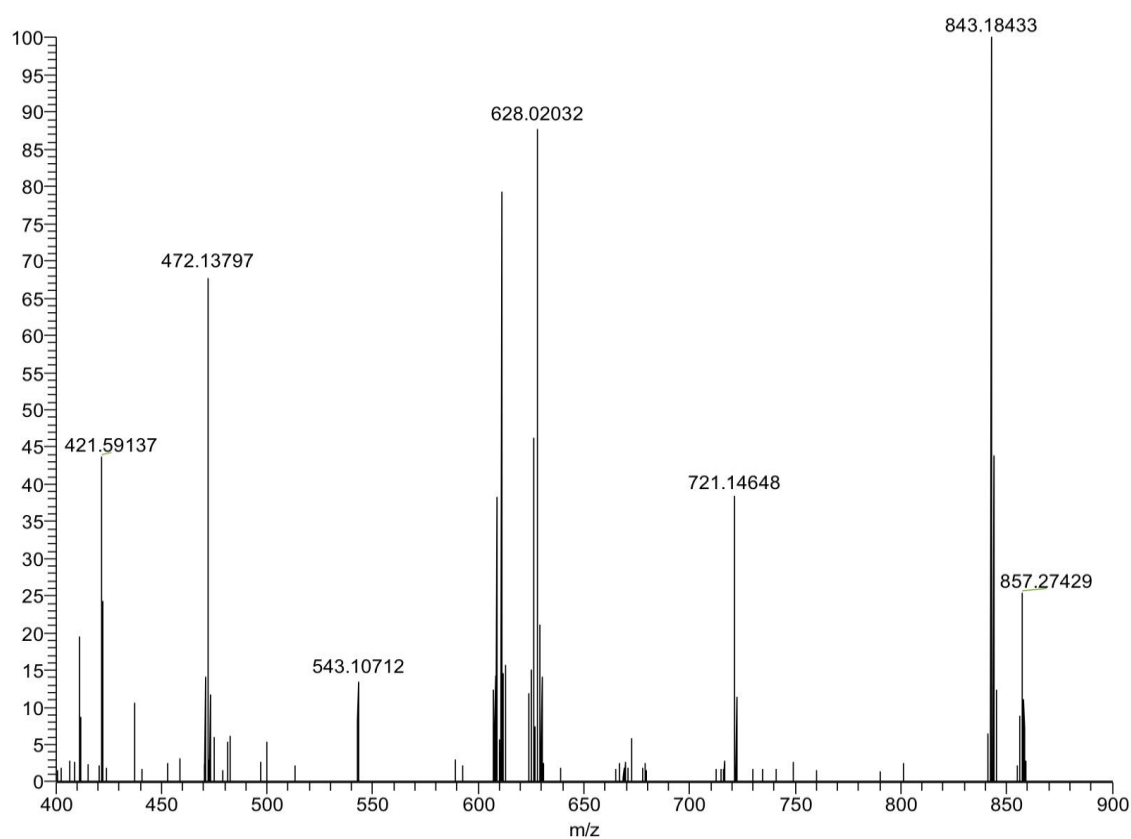


Fig. S 3: Mixture with selenocysteine prepared as above incubated with complex **8** for 3 h at r.t. (only traces left of **8-BF₄**, and no more selenocysteine adduct at 750.05798 left)

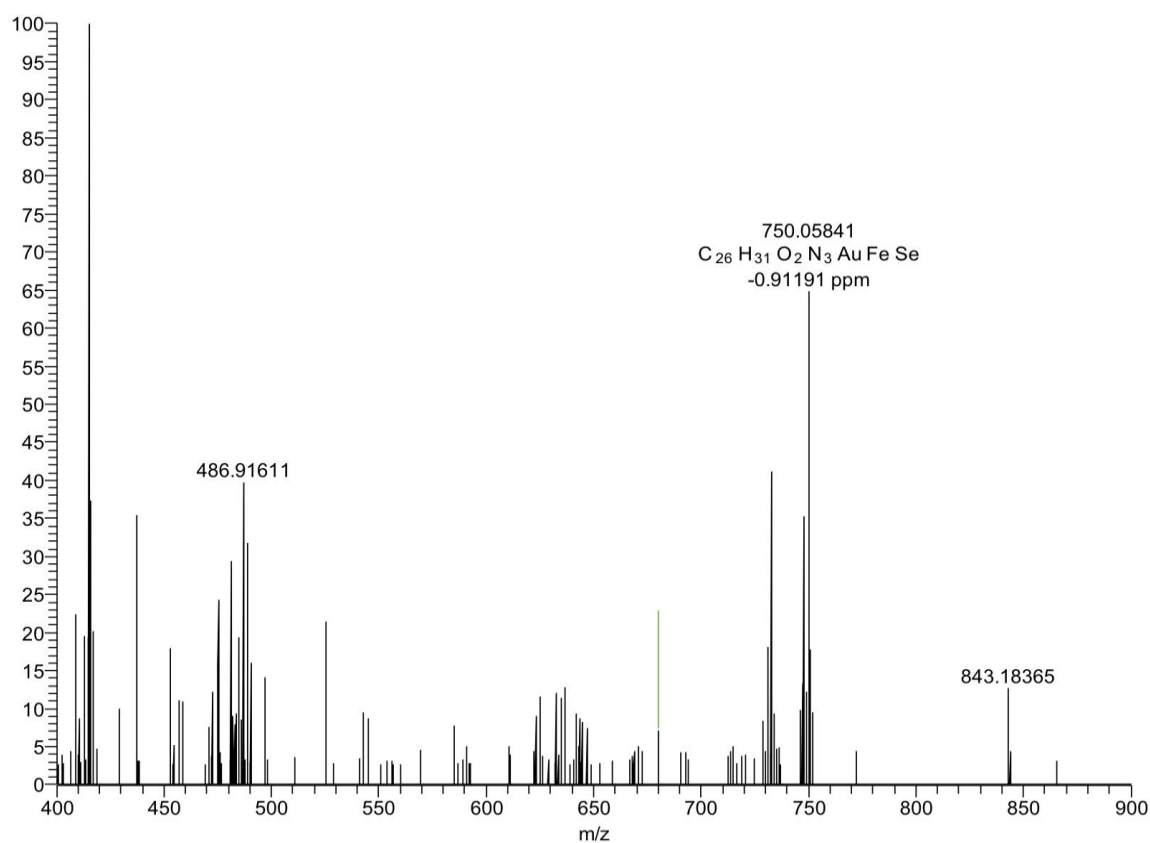


Fig. S 4: Mixture with selenocysteine prepared as above incubated with complex **7b** for 30 min at r.t. (not to scale! same selenocysteine adduct at 750.05798 but far less than with **8**)

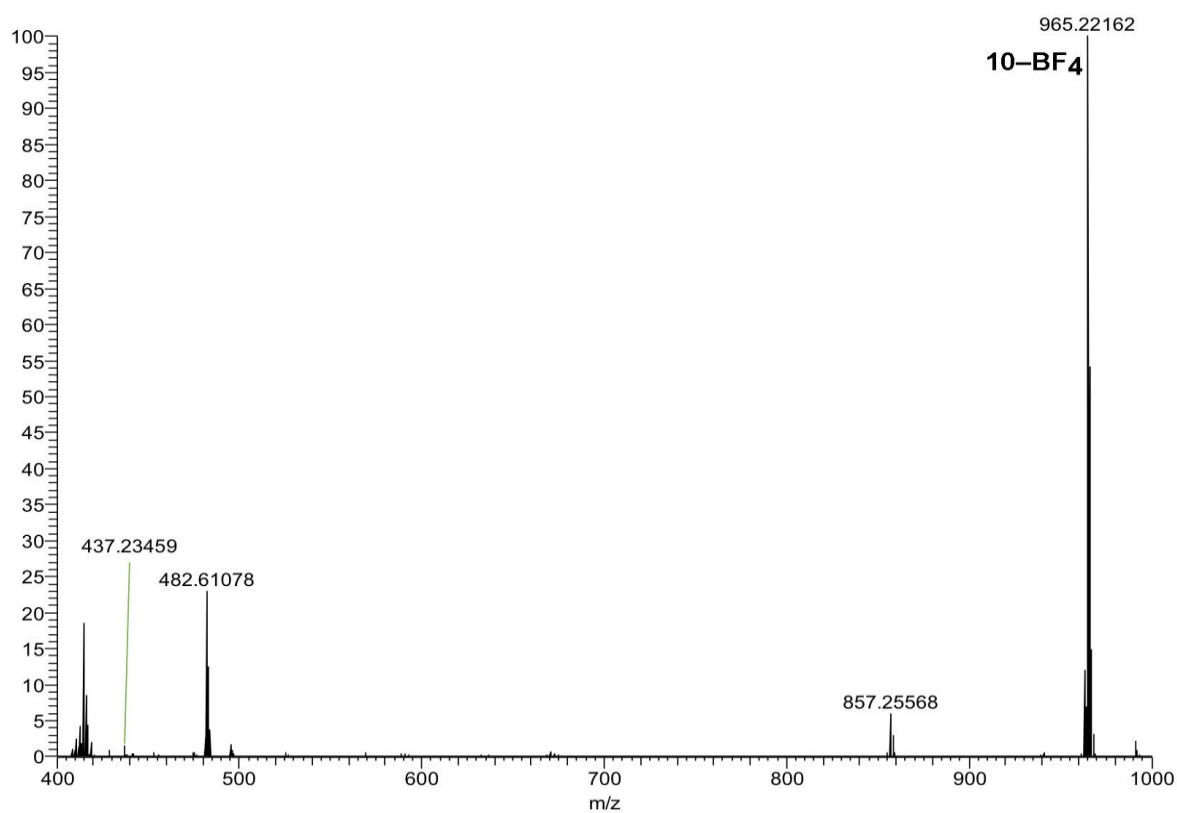


Fig. S 5: Mixture with selenocysteine prepared as above incubated with complex **10** for 30 min at r.t. (no selenocysteine adduct at 750.05798; same negative picture after 6 h!)

Cyclic voltammetry of complex 7b: *Conditions:* Solution in acetonitrile with 0.1 M Bu_4NPF_6 as a conducting salt. Scan rate 50 mV/s. Solid Pt working electrode (cross-section area 0.0314 cm^2 , AMETEK Advanced Measurement Technology); Pt wire as a counter electrode; reference electrode consisting of an Ag wire and AgNO_3 .

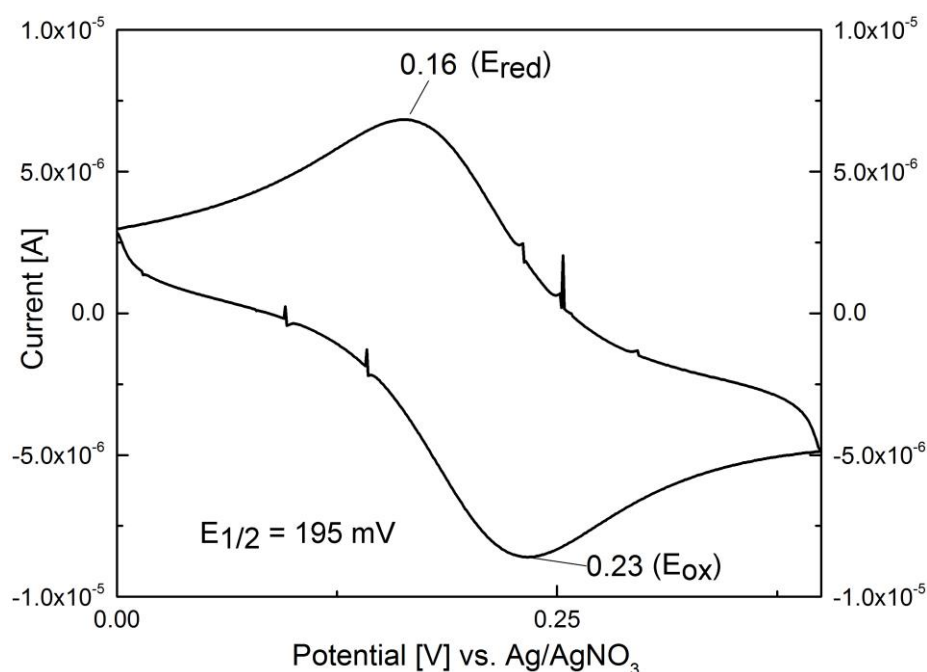


Fig. S 6: cyclic voltammogram of compound **7b**.

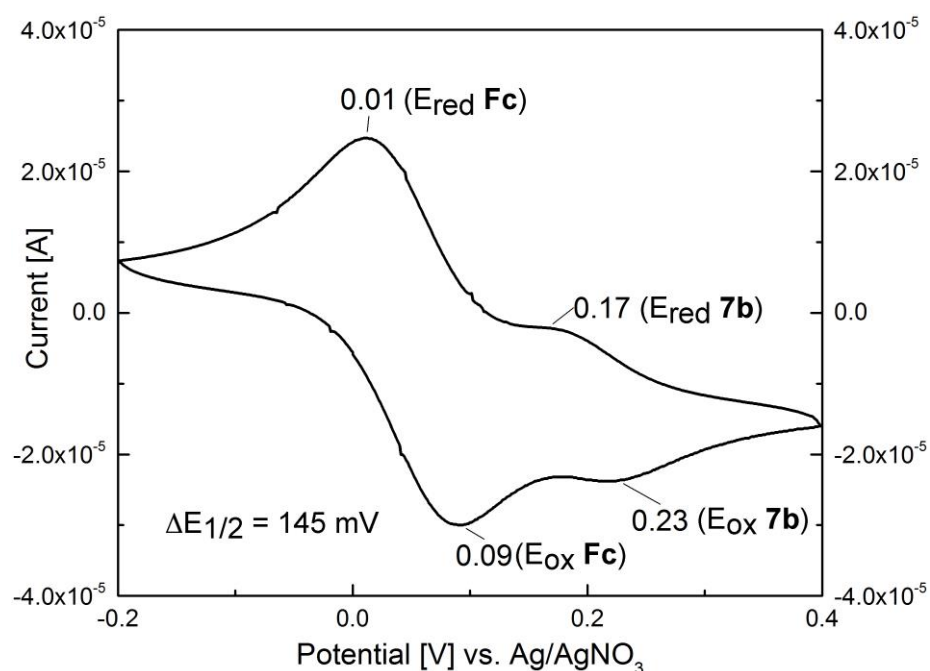


Fig. S 7: cyclic voltammogram of compound **7b** and ferrocene as a reference.

Result: Reversible cyclic voltammogram with $E_{1/2} = 195\text{ mV}$ rel. to $E_{1/2}(\text{ferrocene}) = 50\text{ mV}$. This means an anodic shift of ca 145 mV for the ferrocene unit in complex **7b** rel. to ferrocene.

References

- (1) Jansen, B.; Schlagbauer-Wadl, H.; Eichler, H.-G.; Wolff, K.; van Elsas, A.; Schrier, P. I.; Pehamberger, H. Activated N-Ras Contributes to the Chemoresistance of Human Melanoma in Severe Combined Immunodeficiency (SCID) Mice by Blocking Apoptosis. *Cancer Res.* **1997**, *57* (3), 362–365.
- (2) Versteeg, R.; Noordermeer, I. A.; Krüse-Wolters, M.; Ruiter, D. J.; Schrier, P. I. C-Myc down-Regulates Class I HLA Expression in Human Melanomas. *EMBO J.* **1988**, *7* (4), 1023.
- (3) Selzer, E.; Pimentel, E.; Wacheck, V.; Schlegel, W.; Pehamberger, H.; Jansen, B.; Kodym, R. Effects of Betulinic Acid Alone and in Combination with Irradiation in Human Melanoma Cells. *J. Invest. Dermatol.* **2000**, *114* (5), 935–940.
- (4) Mosmann, T. Rapid Colorimetric Assay for Cellular Growth and Survival: Application to Proliferation and Cytotoxicity Assays. *J. Immunol. Methods* **1983**, *65* (1-2).
- (5) Green, D. R.; Reed, J. C. Mitochondria and Apoptosis. *Science* **1998**, *281* (5381), 1309–1312.
- (6) Salvioli, S.; Ardizzoni, A.; Franceschi, C.; Cossarizza, A. JC-1, but Not DiOC6(3) or Rhodamine 123, Is a Reliable Fluorescent Probe to Assess Delta Psi Changes in Intact Cells: Implications for Studies on Mitochondrial Functionality during Apoptosis. *FEBS Lett.* **1997**, *411* (1).
- (7) Reers, M.; Smiley, S. T.; Mottola-Hartshorn, C.; Chen, A.; Lin, M.; Chen, L. B. Mitochondrial Membrane Potential Monitored by JC-1 Dye. *Methods Enzymol.* **1995**, *260*, 406–417.
- (8) S. M. Meier, C. Gerner, B. K. Keppler, M. A. Cinellu, A. Casini, *Inorg. Chem.* **2016**, *55*, 4248–4259.

NMR Spectra

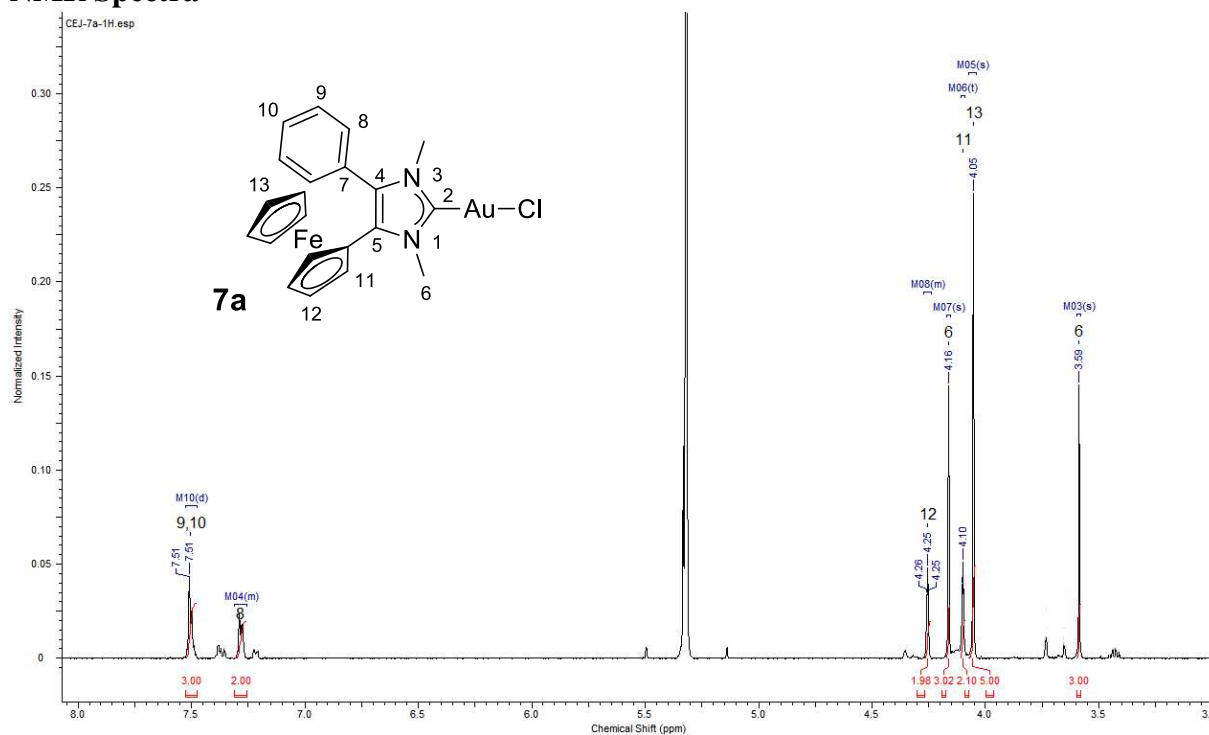


Fig. S 8: ¹H-NMR (CD₂Cl₂, 500 MHz) of complex **7a**.

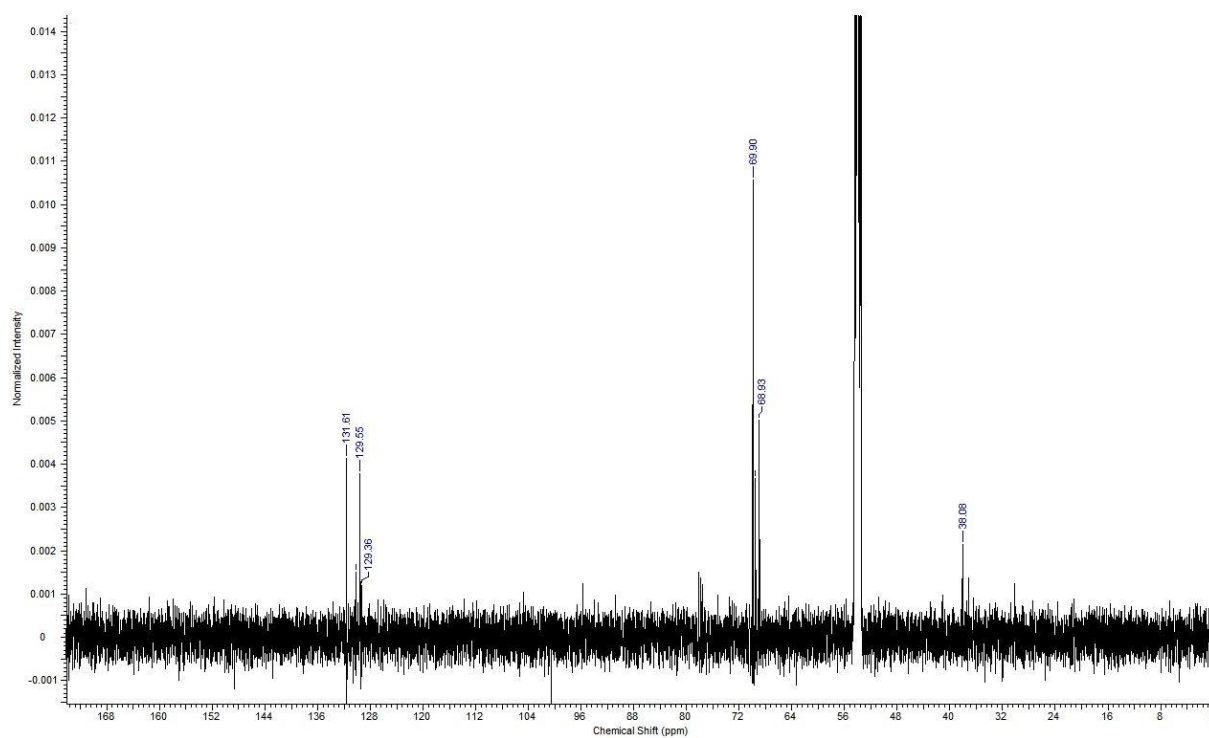


Fig. S 9: ¹³C-NMR (CD₂Cl₂, 125 MHz) of complex **7a**.

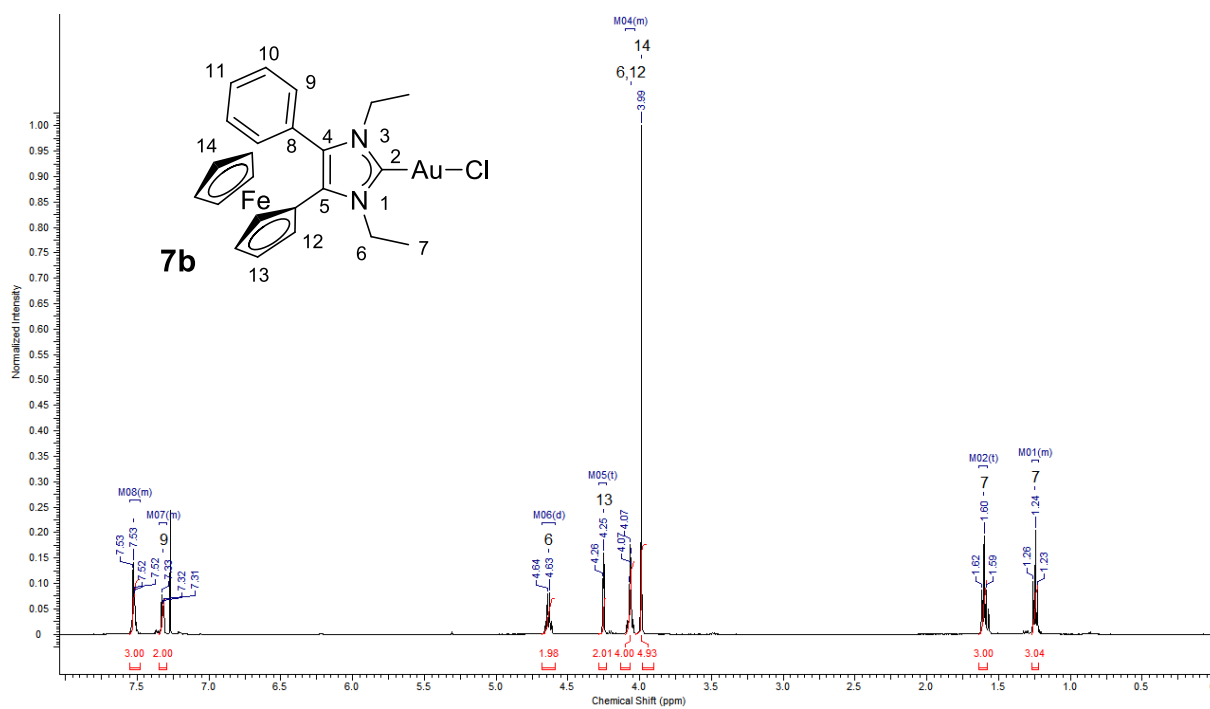


Fig. S 10: $^1\text{H-NMR}$ (CDCl₃, 500 MHz) of complex **7b**.

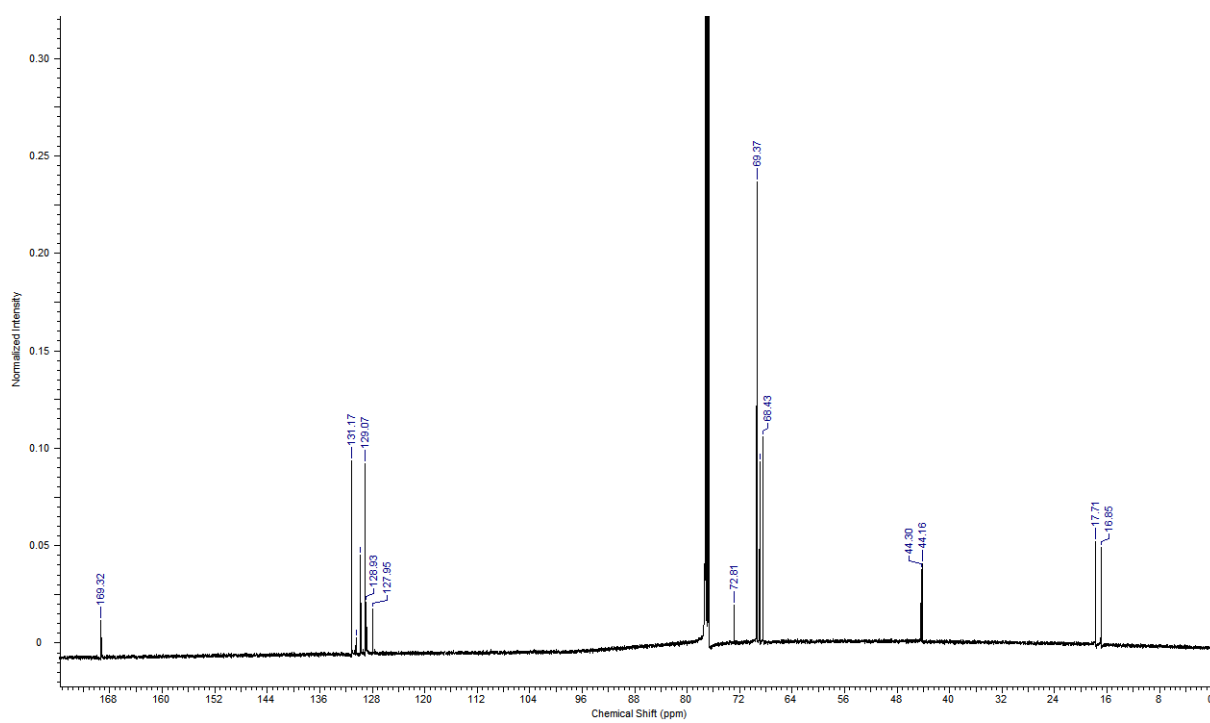


Fig. S 11: $^{13}\text{C-NMR}$ (CDCl₃, 125 MHz) of complex **7b**.

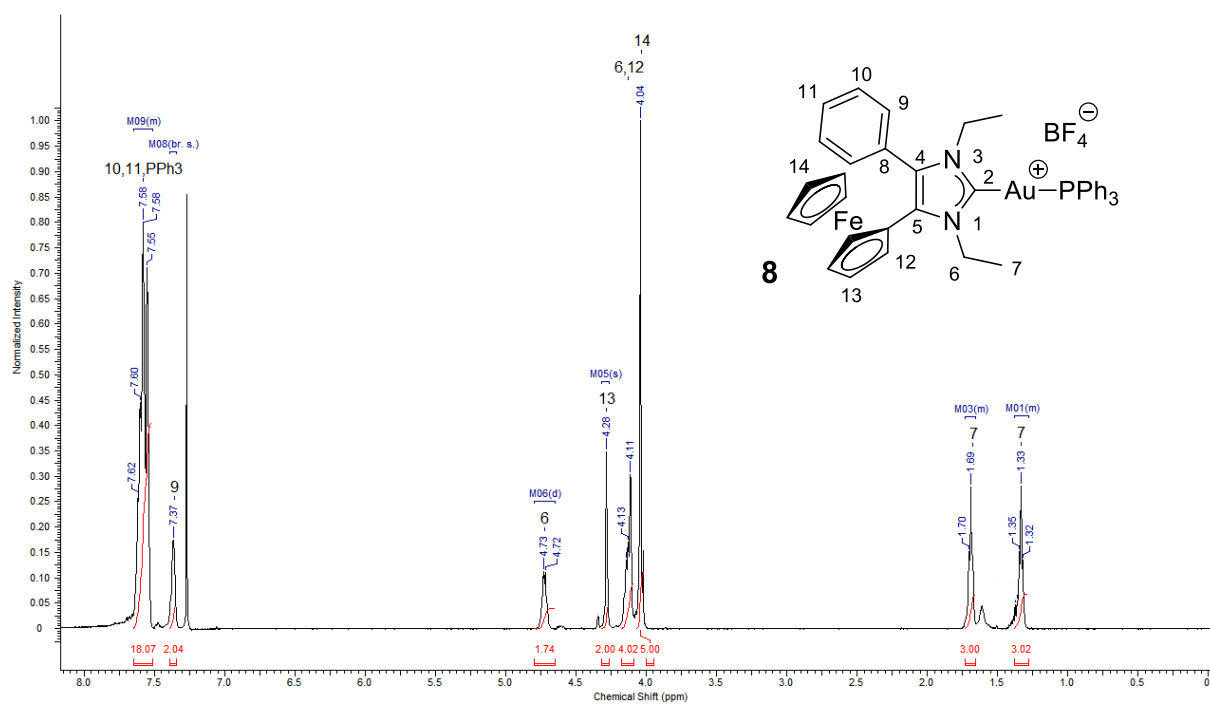


Fig. S 12: ^1H -NMR (CDCl₃, 500 MHz) of complex **8**.

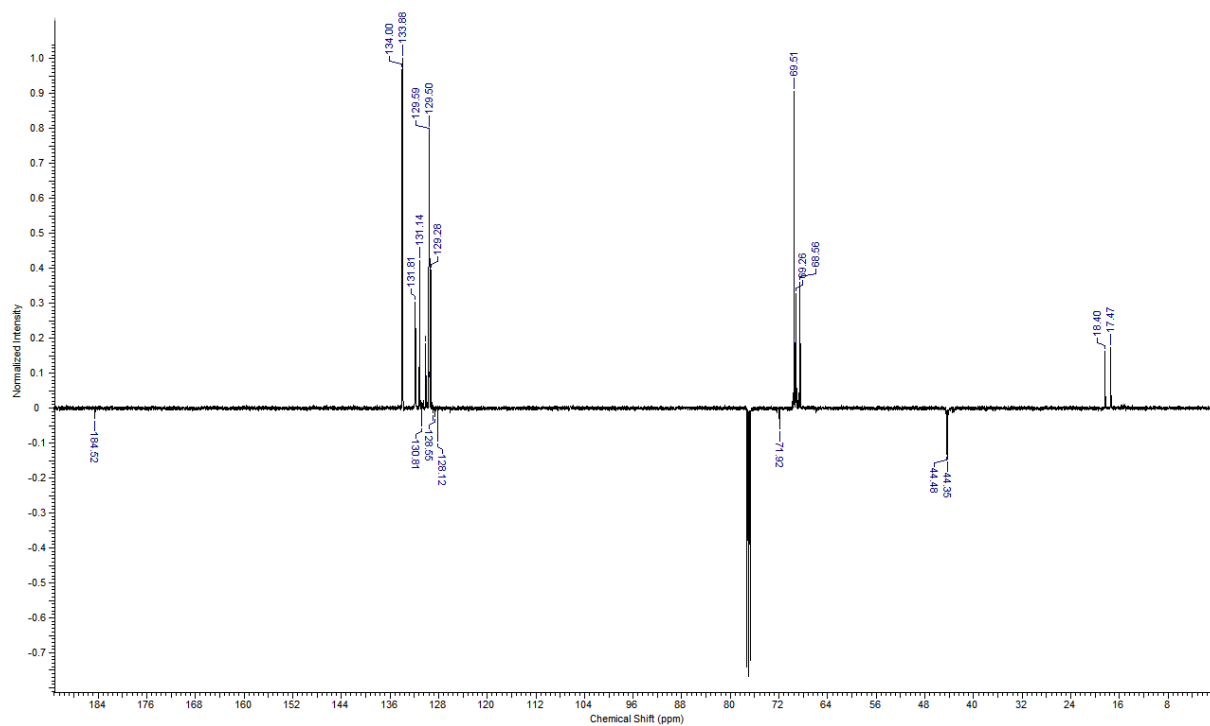


Fig. S 13: ^{13}C -APT-NMR (CDCl₃, 125 MHz) of complex **8**.

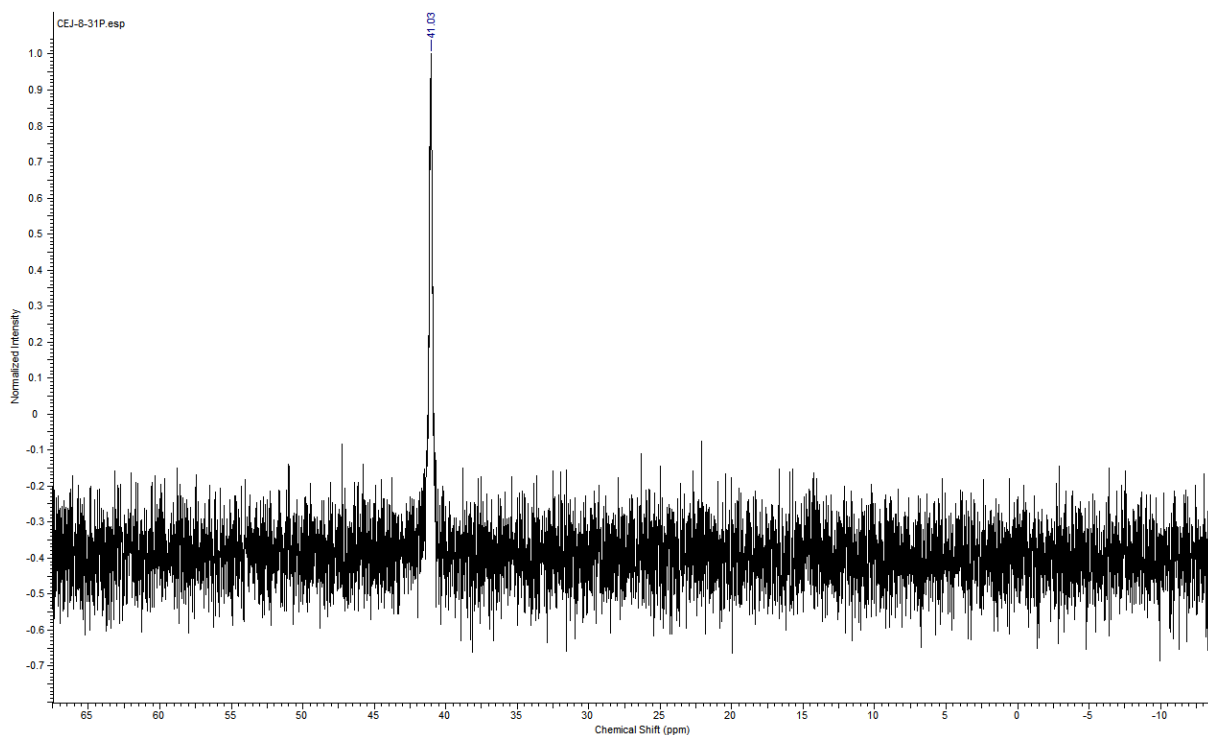


Fig. S 14: ^{31}P -NMR (CDCl_3 , 202 MHz, 85 % phosphoric acid as external reference) of complex **8**.

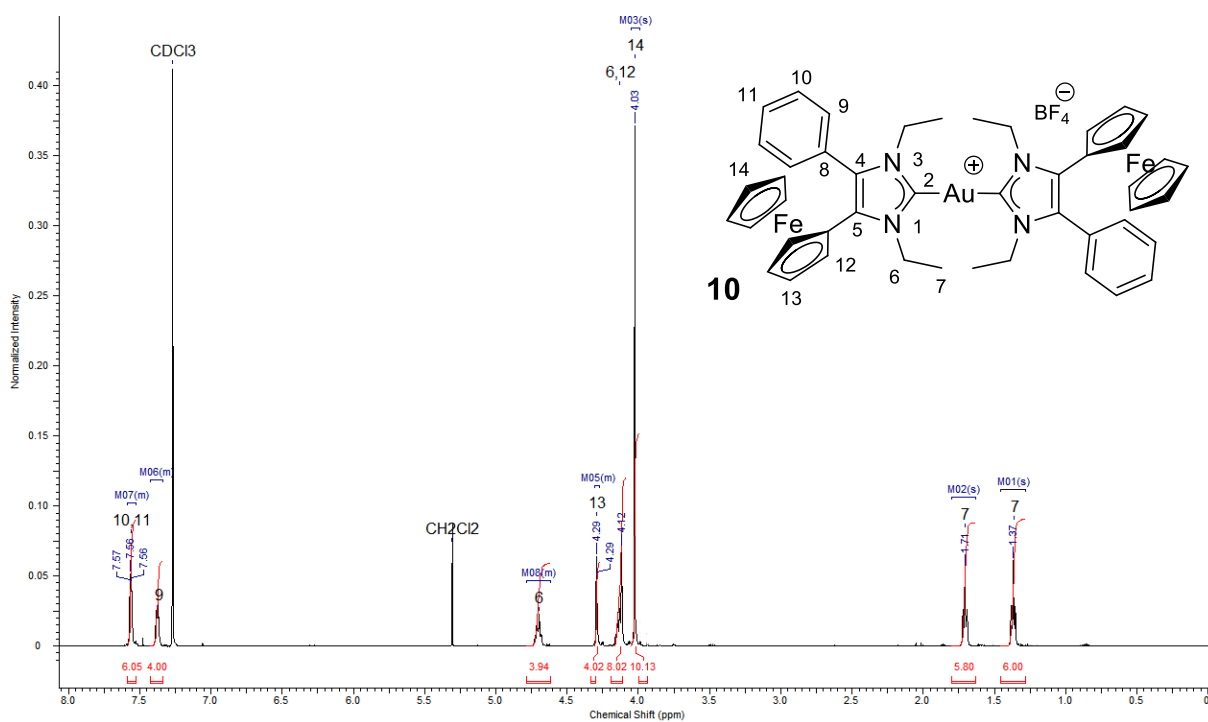


Fig. S 15: ^1H -NMR (CDCl_3 , 500 MHz) of complex **10**.

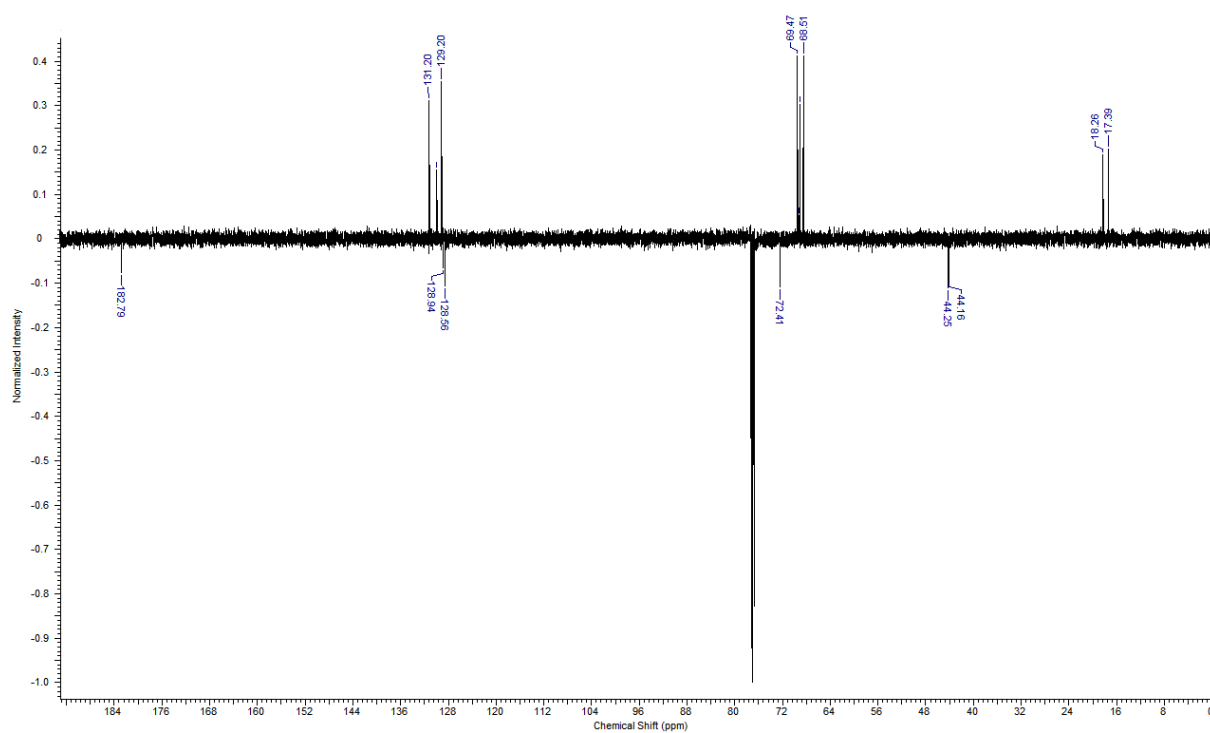


Fig. S 16: ^{13}C -APT-NMR (CDCl_3 , 125 MHz) of complex **10**.